

# Optimal mean first-passage time for a Brownian searcher subjected to resetting: experimental and theoretical results

Benjamin Besga<sup>1</sup>, Alfred Bovon<sup>1</sup>, Artyom Petrosyan<sup>1</sup>, Satya N. Majumdar<sup>2</sup>, Sergio Ciliberto<sup>1\*</sup>

<sup>1</sup> *Univ Lyon, Ens de Lyon, Univ Claude Bernard, CNRS, Laboratoire de Physique, UMR 5672, F-69342 Lyon, France and*

<sup>2</sup> *LPTMS, CNRS, Univ. Paris-Sud, Université Paris-Saclay, UMR 8626, 91405 Orsay, France*

(Dated: April 28, 2020)

We study experimentally and theoretically the optimal mean time needed by a free diffusing Brownian particle to reach a target at a distance  $L$  from an initial position in the presence of resetting. Both the initial position and the resetting position are Gaussian distributed with width  $\sigma$ . We derived and tested two resetting protocols, one with a periodic and one with random (Poissonian) resetting times. We computed and measured the full first-passage probability distribution that displays spectacular spikes immediately after each resetting time for close targets. We study the optimal mean first-passage time as a function of the resetting period/rate for different values of the ratio  $b = L/\sigma$  and find an interesting phase transition at a critical value  $b = b_c$ . For  $b_c < b < \infty$ , there is a *metastable* optimum time which disappears for  $b < b_c$ . The intrinsic difficulties in implementing these protocols in experiments are also discussed.

When searching for a lost object in vain for a while, intuition tells us that maybe one should stop the current search and restart the search process all over again. The rationale behind this intuition is that a restart may help one to explore new pathways, thus facilitating the search process. This intuition has been used empirically before in various stochastic search algorithms (such as simulated annealing) to speed up the search process [1–4]. More recently, in the physics literature, this fact was demonstrated explicitly by studying the mean first-passage time (MFPT) for a single particle (searcher) to a fixed target in various models, in the presence of resetting (for a recent review see [5]).

Searching a target via resetting is an example of the so called intermittent search strategy [6] that consists of a mixture of short-range moves (where the actual search takes place) with intermittent long-range moves where the searcher relocates to a new place and starts a local search in the new place. More precisely, let there be a fixed target at some point in space and a particle (searcher) starts its dynamics from a fixed initial position in space. The dynamics of the particle may be arbitrary, e.g., it may be simply diffusive [7, 8]. Resetting interrupts the natural dynamics of the particle either randomly at a constant rate  $r$  [7, 8] or periodically with a period  $T$  [9, 10], and sends the particle to its initial position. The dynamics starts afresh from the initial position after each resetting event. The MFPT to find a target, located at a fixed distance away from the initial position, typically shows a unique minimum as a function of  $r$  (or  $T$  for periodical resetting). These studies have led to the paradigm that resetting typically makes the search process more efficient and moreover, there often exists an optimal resetting rate  $r^*$  (or period  $T^*$ ) that makes the search time minimal [7, 8].

While this ‘optimal resetting’ paradigm has been tested and verified in a large number of recent theoretical and numerical studies [9, 11–28] (see also the review [5]), to the best of our knowledge it has not been verified experimentally (see however the very recent preprint [29], which appeared in arXiv during the writing of this article, where the authors used a holographic optical tweezer set-up. Their resetting protocols though are quite different from ours). The purpose of this Letter is to report an experimental realization using optical laser traps and subsequent test/verification of this ‘optimal resetting’ paradigm. The goal of the experiment is not just to mimic the theoretical models, but we will see that designing an experiment with a realistic resetting protocol is challenging. Moreover, our experimental protocol led us, in turn, to study new models that exhibit interesting, rich and novel phenomena associated to resetting, namely metastability and phase transition in the MFPT as a function of resetting rate/period.

*Experimental set-up.* We have implemented an optimal search protocol with a Brownian particle which is periodically or randomly reset using an optical tweezers [30]. We use silica micro-sphere of radius  $R = 1 \mu\text{m}$  ( $\pm 5\%$ ) immersed in pure water. The fluid chamber is designed to have very few particles in the measuring volume which allows us to take long measurements. A near infrared laser with wavelength  $\lambda = 1064 \text{ nm}$  is focused into the chamber through an oil immersion objective (Leica  $63\times$  and  $1.4 \text{ NA}$ ) to create an optical trap. The particle is trapped in two dimensions in the  $(x,y)$  plane by a harmonic potential with stiffness  $\kappa$ . The stiffness is controlled by changing the optical power in the chamber directly by laser current modulation (up to  $10 \text{ kHz}$ ) or by means of an electro-optical modulator (EOM).

The position of the particle in the  $(x,y)$  plane can be tracked (see Fig. 1) either by a white light imaging on a camera (maximum speed around  $1000$  frames per second) or from the deviation of a red laser on a quadrant photodiode (QPD) with a band pass around  $1 \text{ MHz}$ . The experiments were performed close to the bottom surface of the cell to avoid errors in position reading due to sedimentation. Henceforth, for simplicity, we will focus only on the  $x$ -component

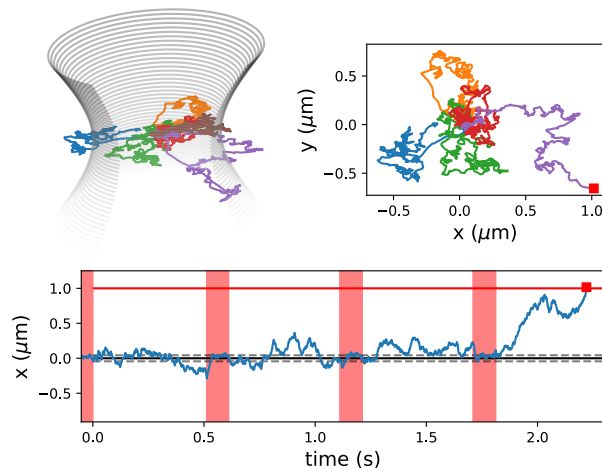


FIG. 1: *Top panel* : Sketch of the optical trap and a Brownian trajectory in the 2D plane  $(x,y)$  with resetting. *Bottom panel* : typical 1D Brownian trajectory with periodic resetting (red colored area) at time  $T = 0.5$  s. The equilibrium standard deviation of the trapped particle  $\sigma = 43$  nm is shown (dotted lines). The target (red square  $1 \mu\text{m}$  away from the center of the trap) is reached when  $x$  crosses the red line for the first time.

of the particle's position, i.e., the one dimensional trajectory. We can thus follow the particle position during its free diffusion and after a time  $T$  reset its position by turning on the optical trap which allows us to realize different protocols.

*Periodic resetting protocol.* The experimental protocol leads us to study a model of diffusion in (effectively) one dimension subjected to periodic resetting. We consider an overdamped particle in thermal equilibrium inside a harmonic trap with potential  $U(x) = \kappa x^2/2$ , where the stiffness  $\kappa$  is proportional to the trapping laser power. This means that the initial position  $x_0$  is distributed via the Gibbs-Boltzmann distribution which is simply Gaussian:  $\mathcal{P}(x_0) = e^{-x_0^2/2\sigma^2}/\sqrt{2\pi\sigma^2}$  where the width  $\sigma = \sqrt{k_B T/\kappa}$ . We also consider a fixed target at location  $L$ . At time  $t = 0$ , the trap is switched off for an interval  $T$  and the particle undergoes free diffusion (overdamped) with diffusion constant  $D = k_B T/\Gamma$  (here  $\Gamma$  denotes the damping constant). At the end of the period, the particle's position is reset (see Fig. 1). Performing the resetting of the position poses the real experimental challenge.

In standard models of resetting one usually assumes instantaneous resetting [5], which is however impossible to achieve experimentally. There have been recent theoretical studies that incorporates a 'refraction' period before the particle's position is reset [20, 31–33]. In our experiment, we have an analogue of this refraction period: after the period  $T$ , we switch on the optimal harmonic trap and we let the particle relax back to its equilibrium thermal distribution. This relaxation can, in principle, be made arbitrarily fast using, e.g., the recently developed 'Engineered Swift Equilibration' (ESE) technique [34–38]. In our experiment we determine the characteristic relaxation time  $\tau_c$  and during the period  $[T, T + \tau_{\text{eq}}]$  with  $\tau_{\text{eq}} \simeq 3\tau_c$ , we do not make any measurement. In other words, even if the particle encounters the target during the relaxation period, we do not count that event as a first-passage event. Thus in this set-up, the thermal relaxation mimics the instantaneous resetting, with one major difference however. We do not reset it to exactly the same initial position, rather the new 'initial' position at the end of the time epoch  $T + \tau_{\text{eq}}$  is drawn from the Gibbs-Boltzmann distribution  $\mathcal{P}(x_0)$ . At time  $T + \tau_{\text{eq}}$ , we again switch off the trap and we let the particle diffuse freely for another period  $T$ , followed by the thermal relaxation over period  $\tau_{\text{eq}}$ . The process repeats periodically. During the free diffusion, if the particle finds the target at  $L$ , we measure the first-passage time  $t_f$ . Note that the first-passage time  $t_f$  is the net 'diffusion' time spent by the particle before reaching the target (not counting the intermediate relaxation periods  $\tau_{\text{eq}}$ ). Averaging over many realizations, we then compute the MFPT  $\langle t_f \rangle$ , for fixed target location  $L$  and fixed resetting period  $T$ .

The MFPT for this protocol can be computed exactly, as detailed in the Supp. Mat. [39]. Our main result can be summarized in terms of two dimensionless quantities

$$b = \frac{L}{\sigma}; \quad \text{and} \quad c = \frac{L}{\sqrt{4DT}}. \quad (1)$$

The parameter  $b$  quantifies how far the target is from the center of the trap in units of the trapped equilibrium standard deviation. The second parameter  $c$  tells us how fast we reset the particle compared to its free diffusion time.

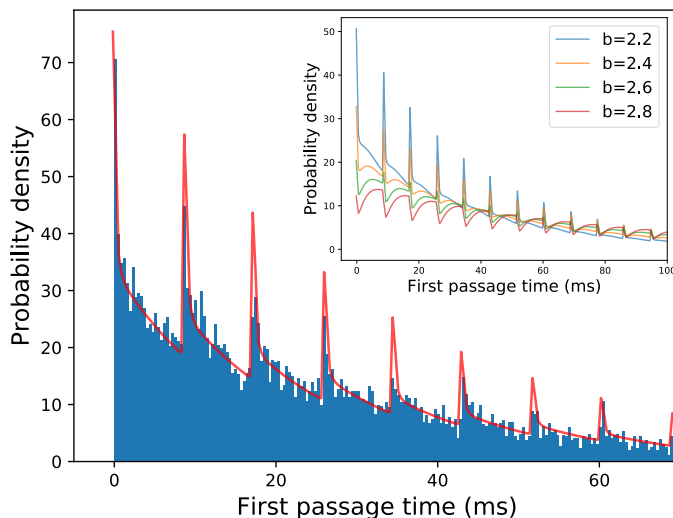


FIG. 2: Experimental (blue histogram) and theoretical (red line) PDF  $F(t)$  of the first-passage time. We measured  $1.2 \times 10^4$  first-passage times for  $b = 2$  and  $c = 1$  ( $T = 8.6$  ms). The spikes occur just immediately after  $t = nT$  where  $n = 0, 1, 2, \dots$ . *Inset*: The PDF  $F(t)$  vs.  $t$  (theoretical) for  $b = 2.2$  to  $2.8$  that demonstrates that the spikes disappear rapidly with increasing  $b$ . The PDF  $F(t)$  is normalized such that  $\int_0^\infty F(t)dt = 1$  with  $dt = 3.5 \times 10^{-4}$  s.

We show that the dimensionless MFPT  $\tau$  can be expressed as a function of these two parameters  $b$  and  $c$

$$\tau = \frac{4D\langle t_f \rangle}{L^2} = w(b, c), \quad (2)$$

where

$$w(b, c) = \frac{\int_0^1 dv \int_{-\infty}^{\infty} du e^{-u^2/2} \operatorname{erf}\left(\frac{c}{\sqrt{v}}|1 - u/b|\right)}{c^2 \int_{-\infty}^{\infty} du e^{-u^2/2} \operatorname{erfc}(c|1 - u/b|)}. \quad (3)$$

While it is hard to evaluate the integrals explicitly,  $w(b, c)$  can be easily plotted numerically to study its dependence on  $b$  and  $c$ , as discussed later. Going beyond the first moment  $\langle t_f \rangle$  and computing the full probability density function (PDF) of the first-passage time  $t_f$  is also of great interest [40–43]. Indeed, we computed the PDF  $F(t)$  of  $t_f$  (see [39]) and the result is plotted in Fig. (2). For small  $b$ , we found striking spikes in  $F(t)$  just after each resetting event. We show in [39] that setting  $t = nT + \Delta$  with  $n = 0, 1, 2, \dots$  and  $\Delta \rightarrow 0^+$ , the first-passage density  $F(t = nT + \Delta)$  displays a power law divergence (the spikes) as  $\Delta \rightarrow 0^+$

$$F(t = nT + \tau) \simeq A_n(b) \Delta^{-1/2} \quad (4)$$

with an amplitude  $A_n(b)$  that can be computed explicitly [39]. We find that as  $b$  increases,  $A_n(b)$  decays rapidly and the spikes disappear for large  $b = L/\sigma$  (see the inset of Fig. (2)). Instead for large  $b$ ,  $F(t)$  drops by a finite amount after each period (as seen in the inset). In theoretical models of resetting to a fixed initial position ( $\sigma = 0$  or  $b \rightarrow \infty$ ), these spikes are completely absent and hence they constitute clear signatures of the finiteness of  $\sigma$ . Physically, these spikes occur for finite  $\sigma$  because each resetting event enhances the probability to find the target without the need of diffusion.

In order to test experimentally these results we realized a periodic resetting protocol and measure the statistics of first-passage times. The diffusion coefficient (typically  $D \simeq 2.10^{-13}$  m<sup>2</sup>/s) is measured during the free diffusion part and the width of the Gaussian (typically  $\sigma \simeq 40$  nm) when the particle is back to equilibrium. These independent and simultaneous measures allow us to overcome experimental drifts. In figure 2 we show the experimentally obtained PDF of  $10^4$  measured first-passage times for  $b = 2$  and  $c = 1$ . We also compared with our theoretical prediction [39]. We observe a very good agreement with no free parameter.

To analyse the MFPT, we start with the limit  $b \gg 1$  of Eq. (3), i.e.,  $L \gg \sigma$ . This limit corresponds to the case when the target is much farther away compared to the typical fluctuation of the initial position. In this case, taking

$b \rightarrow \infty$  limit in Eq. (3) we get

$$w(c) = w(b \rightarrow \infty, c) = \frac{\text{erf}(c) + 2c \left( e^{-c^2} / \sqrt{\pi} - c \text{erfc}(c) \right)}{c^2 \text{erfc}(c)}, \quad (5)$$

where  $\text{erf}(c) = (2/\sqrt{\pi}) \int_0^c e^{-u^2} du$  and  $\text{erfc}(c) = 1 - \text{erf}(c)$ . In Fig. (3), we plot  $w(c)$  vs  $c$  and compare with our experimental data and find good agreement with no adjustable parameter. Typically a few thousands of first-passage events (several hours of measurements) are needed to have a good estimate of the MFPT given the slowly decaying distribution of the first-passage times. The standard deviation of first-passage times is indeed of the same order as the MFPT. We see a distinct optimal value around  $c^* = 0.74$ , at which  $w(c^*) = 5.3$ . Our results thus provide a clear experimental verification of this optimal resetting paradigm. Let us remark that the authors in Ref. [9] studied periodic resetting to the fixed initial position  $x_0 = 0$  and obtained the MFPT by a different method than ours. Our  $b \rightarrow \infty$  limit result in Eq. (5) indeed coincides with that of [9], since when  $\sigma \ll L$ , our protocol mimics approximately a resetting to the origin.

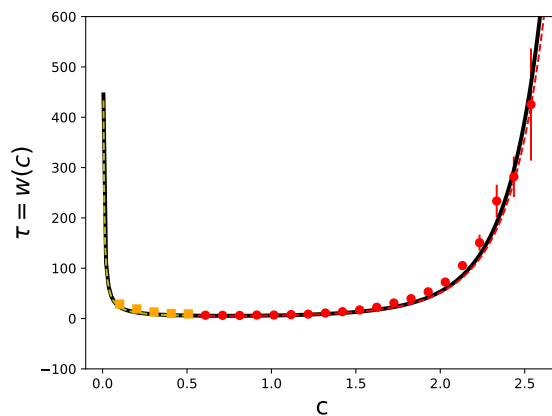


FIG. 3:  $w(c) \equiv w(b \rightarrow \infty, c)$  vs.  $c$  curve. The solid black line represents the theoretical formula for  $w(c)$  in Eq. (5), while the dots denote the experimental data with  $b = 30$  (red dots) and  $b = 5$  (yellow square). The dotted lines shows  $w(b, c)$  with  $b = 5$  for small  $c$  in yellow, and with  $b = 30$  for higher  $c$  in red. The error bars are given by the standard deviation of the MFPT distribution divided by the square root of the number of events.

What happens when  $b = L/\sigma$  is finite? Remarkably, when we plot  $w(b, c)$  in Eq. (3) as a function of  $c$  for different fixed values of  $b$ , we see that  $w(b, c)$  decreases as  $c$  increases, indeed achieves a minimum at  $c_1(b)$ , then increases, achieves a maximum at  $c_2(b)$  and then decreases monotonically as  $c$  increases beyond  $c_2(b)$  (see Fig. (4)). When  $b \rightarrow \infty$ , the maximum at  $c_2(b) \rightarrow \infty$  and one has a true minimum. However, for finite  $b$ , the “optimal” (minimal) MFPT at  $c = c_1$  is thus actually a metastable minimum and the true minimum occurs at  $c \rightarrow \infty$ , i.e., when the resetting period  $T \rightarrow 0$ . Physically, the limit  $T \rightarrow 0$  corresponds to repeated (almost continuously) resetting and since the target position and the initial location are of the same order, the particle may find the target simply by resetting, without the need to diffuse. Interestingly, this metastable minimum exists only for  $b > b_c \approx 2.3$ . When  $b < b_c$ , the curve  $w(b, c)$  decreases monotonically with  $c$  and there is only a single minimum at  $c \rightarrow \infty$ , or equivalently for  $T \rightarrow 0$ . Thus the system undergoes a “first-order” phase transition as  $b = L/\sigma$  is tuned across a critical value  $b_c \approx 2.3$ , from a phase with a metastable optimum at a finite  $c = c_1(b)$  to one where the only minimum occurs at  $c \rightarrow \infty$ . This phase transition is well reproduced by the experimental data points. The deviation from theoretical prediction for high values of  $c$  is due to the limited experimental acquisition rate (here 50000 Hz) that prevents us from detecting very fast events and thus leads to an overestimation of the MFPT as confirmed by our numerical simulations. This phase transition was rather unexpected and came out as a surprise.

*Random resetting protocol.* It turns out that this metastability and the phase transition is rather robust and exists for other protocols, such as Poissonian resetting where the resetting occurs at a constant rate  $r$ . Here, the dimensionless variables are  $b = L/\sigma$  and  $c = \sqrt{r/D} L$  and the scaled MFPT  $\tau = 4D\langle t_f \rangle / L^2$  again becomes a function  $w_2(b, c)$  of  $b$  and  $c$  (analogue of Eq. (3)). In this case, we get a long but explicit  $w_2(b, c)$  (see [39] for details). In Fig. (5) we plot  $w_2(b, c)$  vs.  $c$  for different values of  $b$  together with experimental data. We have a good agreement between theory and experiment and here again the deviation at high  $c$  comes from limited experimental acquisition

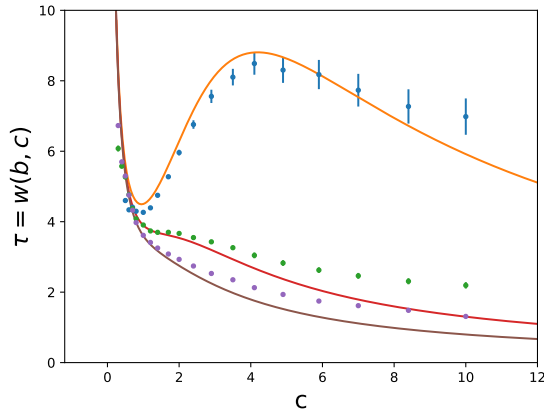


FIG. 4: The scaled MFPT  $\tau = w(b, c)$  vs.  $c$  curves and experimental data for  $b = 3$  (orange curve and blue dots),  $b = 2.3$  (red curve and green dots) and  $b = 2$  (brown curve and purple dots), for the periodic resetting protocol. The theoretical curves are obtained from Eq. (3). The scaled MFPT has two different behavior depending on how far is the target. If  $b > b_c \approx 2.3$  the MFPT  $\tau$  exhibits a local minimum, whereas it decreases monotonically for  $b$  lower than the critical value  $b_c$ .

rate. Once again we see that there is a metastable minimum that disappears when  $b$  decreases below a critical value  $b_c \approx 2.53$ . When  $b \rightarrow \infty$ , there is only a single minimum at  $c^* = 1.59362$  where  $w_2(\infty, c^*) = 6.17655$ . Thus this phenomenon of metastability and phase transition in MFPT seems to be robust.

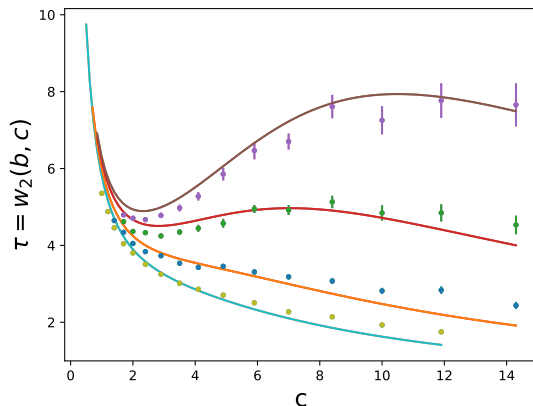


FIG. 5: Scaled MFPT  $\tau = w_2(b, c)$  vs  $c$  curves and experimental data points for  $b = 2, 2.3, 2.7$  and  $3$  (from bottom to top) in the case of Poissonian resetting. The metastable minimum disappears for  $b < b_c \approx 2.53$ .

*Conclusions* : We have studied both theoretically and experimentally the role of the variance of the resetting position on the optimal time needed for a Brownian bead to reach a specific immobile target. We have applied two different protocols, one with a periodic and another with a random resetting time. We found that both present a metastable minimum for  $b > b_c$  (where  $b_c$  depends on the protocol), showing that this transition could be a universal feature of MFPT protocols for resetting. For the periodic protocol, we also computed and measured the full PDF of the first-passage time and found that it displays striking spikes after each resetting event, a clear effect of the finiteness of the variance of the initial position. The experimental data agree well with theoretical predictions, but the experiment is not a mere test of the theory. Indeed we point out a series of experimental difficulties that one has to consider when one applies such theoretical predictions in real systems. On one side when the particle is free for a very long time (small  $c$ ) there are problems of sedimentation that must be taken into account because they may influence a lot the final result. On the very short times (large  $c$ ) we have shown that finite sampling time affects the results, because if the first-passage is not detected, it leads to an overestimation of the first-passage time. It is clear

that at very fast sampling rate the model will fail and probably the role of inertia, which has been always neglected, should be taken into account in future theoretical developments.

We thank E. Trizac for useful discussions. SNM wants to thank the warm hospitality of ICTS (Bangalore) where this work was completed.

---

\* E-mail me at: [sergio.ciliberto@ens-lyon.fr](mailto:sergio.ciliberto@ens-lyon.fr)

- [1] M. Villen-Altramirano and J. Villen-Altramirano, *RESTART: A method for accelerating rare event simulations* (in *Queueing Performance and Control in ATM*, Ed. J. W. Cohen and C. D. Pack (1991)).
- [2] M. Luby, A. Sinclair and D. Zuckerman, *Optimal speedup of Las Vegas algorithms*, Inf. Proc. Lett. **47** 4391 (1993).
- [3] H. Tong, C. Faloutsos, and J-Y. Pan *Random walk with restart: fast solutions and applications* Knowl. Inf. Syst. **14** 327 (2008).
- [4] J. H. Lorenz *Runtime Distributions and Criteria for Restarts* (in Tjoa A., Bellatreche L., Biffi S., van Leeuwen J., Wiedermann J. (eds) SOFSEM 2018: Theory and Practice of Computer Science. SOFSEM 2018. Lecture Notes in Computer Science, vol 10706, 2018).
- [5] M. R. Evans, S. N. Majumdar, and G. Schehr, J. Phys. A: Math. Theor. **53**, 193001 (2020).
- [6] O. Bénichou O, C. Loverdo, M. Moreau, and R. Voituriez, Rev. Mod. Phys. **83**, 81 (2011).
- [7] M. R. Evans and S. N. Majumdar, Phys. Rev. Lett. **106**, 160601 (2011).
- [8] M. R. Evans and S. N. Majumdar, J. Phys. A: Math. Theor. **44**, 435001 (2011).
- [9] A. Pal, A. Kundu, and M. R. Evans, J. Phys. A: Math. Theor. **49**, 225001 (2016).
- [10] U. Bhat, C. De Bacco, and S. Redner, J. Stat. Mech. **083401** (2016).
- [11] M. R. Evans, S. N. Majumdar and K. Mallick J. Phys. A: Math. Theor. **46**, 185001 (2013).
- [12] M. Montero and J. Villarroel, Phys. Rev. E **87**, 012116 (2013).
- [13] M. R. Evans and S. N. Majumdar, J. Phys. A: Math. Theor. **47**, 285001 (2014).
- [14] L. Kuśmierz, S. N. Majumdar, S. Sabhapandit, and G. Schehr, Phys. Rev. Lett. **113**, 220602 (2014).
- [15] S. Reuveni, M. Urbakh, and J. Klafter, Proc. Natl. Acad. Sci. USA **111**, 4391 (2014).
- [16] T. Rotbart, S. Reuveni, and M. Urbakh, Phys. Rev. E **92** 060101(R) (2015).
- [17] C. Christou C and A. Schadschneider J. Phys. A: Math. Theor. **48**, 285003 (2015).
- [18] L. Kuśmierz and E. Gudowska-Nowak Phys. Rev. E **92** 052127 (2015).
- [19] A. Nagar and S. Gupta S, Phys. Rev. E **93**, 060102 (R) (2016).
- [20] S. Reuveni, Phys. Rev. Lett. **116**, 170601 (2016).
- [21] A. Pal and S. Reuveni, Phys. Rev. Lett. **118**, 030603 (2017).
- [22] A. Chechkin and I. M. Sokolov Phys. Rev. Lett. **121**, 050601 (2018).
- [23] S. Belan, Phys. Rev. Lett. **120**, 080601 (2018).
- [24] M. R. Evans and S. N. Majumdar, J. Phys. A: Math. Theor. **51** 475003 (2018).
- [25] A. Masó-Puigdellosas, D. Campos, and V. Méndez, Phys. Rev. E **99**, 012141 (2019).
- [26] J. Masoliver and M. Montero, Phys. Rev. E **100** 042103 (2019).
- [27] X. Durang, S. Lee, L. Lizana and J-H. Jeon, J. Phys. A: Math. Theor. **52** 224001 (2019).
- [28] A. Pal and V. V. Prasad, Phys. Rev. E **99**, 032123 (2019).
- [29] O. Tal-Friedman, A. Pal, A. Sekhon, S. Reuveni and Y. Roichman, arXiv:2003.03096 (2020).
- [30] A. Bèrut, A. Imparato, A. Petrosyan, and S. Ciliberto. J. Stat. Mech., page P054002, (2016).
- [31] M. R. Evans and S.N. Majumdar, J. Phys. A: Math. Theor. v-52, 01LT01 (2019).
- [32] A. Pal, L. Kusmierz, and S. Reuveni, arXiv: 1907.12208, see also arXiv: 1907.13453
- [33] D. Gupta, C. A. Plata, and A. Pal, arXiv:1909.08512
- [34] I. A. Martinez, A. Petrosyan, D. Guery-Odelin, E. Trizac, and S. Ciliberto, Nature physics, **12**, 843 (2016).
- [35] D. Guery-Odelin, A. Ruschhaupt, A. Kiely, E. Torrontegui, S. Martinez-Garaot, and J. G. Muga, Rev. Mod. Phys., **91**, 045001 (2019).
- [36] C. A. Plata, D. Guery-Odelin, E. Trizac, and A. Prados, Physical Review E, **99**, 012140 (2019).
- [37] D. Gupta, C. A. Plata, and A. Pal, arXiv: 1909.08512
- [38] M. Chupeau, B. Besga, D. Guery-Odelin, E. Trizac, A. Petrosyan, and S. Ciliberto Phys. Rev. E **98**, 010104(R)
- [39] Supplementary Material: We give the details on how the theoretical predictions plotted in Figs. 2), 3) and 4) have been obtained, both for periodic and random resetting.
- [40] S. N. Majumdar, Curr. Sci. **77**, 370 (1999).
- [41] S. Redner, *A guide to first-passage processes*, Cambridge University Press (2001).
- [42] S. N. Majumdar, Physica A, **389**, 4299 (2010).
- [43] A. J. Bray, S. N. Majumdar, and G. Schehr, Adv. in Phys. **62**, 225 (2013).

# Supplementary Material of the Letter: Optimal mean first-passage time for a Brownian searcher subjected to resetting: experimental and theoretical results

Benjamin Besga<sup>1</sup>, Alfred Bovon<sup>1</sup>, Artyom Petrosyan<sup>1</sup>, Satya N. Majumdar<sup>2</sup>, Sergio Ciliberto<sup>1\*</sup>

<sup>1</sup> *Univ Lyon, Ens de Lyon, Univ Claude Bernard, CNRS,*

*Laboratoire de Physique, UMR 5672, F-69342 Lyon, France and*

<sup>2</sup> *LPTMS, CNRS, Univ. Paris-Sud, Université Paris-Saclay, UMR 8626, 91405 Orsay, France*

(Dated: April 28, 2020)

We give the principal details of the theoretical calculations described in the main text of the Letter.

## I. INTRODUCTION

In this supplementary material of the Letter, we give the details on how the theoretical predictions plotted in Figs. 2), 3) and 4) of the main text have been obtained, both for periodic and random resetting protocols. As already pointed out in the main text we consider here a realistic situation in which the initial position at the beginning of each free diffusion period (between successive resetting events) has a Gaussian distribution of width  $\sigma$ . The mean first-passage time (MFPT), in the presence of resetting for either of the two protocols, was previously computed only for the resetting to a fixed initial position  $x_0$  [1–5]. In practice this is not possible to realize experimentally because of the finite stiffness  $\kappa$  of the trap which resets the particle to the initial position. In an optical trap at temperature  $T$ , the resetting position is always Gaussian distributed with a finite variance  $\sigma^2 = k_B T / \kappa$  given by equipartition. As  $\kappa$  is proportional to the laser intensity starting with  $\sigma = 0$  would imply to trap with an infinite power which is of course not possible. Thus we study here the influence of a finite nonzero  $\sigma$  on MFPT.

Consider a searcher undergoing a generic stochastic dynamics starting, say, at the initial position  $x_0$ . The immobile target is located at  $x = L$ . To compute the MFPT of a generic stochastic process, it is most convenient to first compute the survival probability or persistence [6–9]  $S(t|x_0)$ , starting from  $x_0$ . This is simply the probability that the searcher, starting its dynamics at  $x_0$  at  $t = 0$ , does not find the target up to time  $t$ . The first-passage probability density  $F(t|x_0)$  denotes the probability density to find the target for the first time at  $t$ . The two quantities  $F(t|x_0)$  and  $S(t|x_0)$  are simply related to each other via  $S(t|x_0) = \int_t^\infty F(t'|x_0) dt'$ , because if the target is not found up to  $t$ , the first-passage time must occur after  $t$ . Taking a derivative with respect to  $t$  gives

$$F(t|x_0) = -\frac{dS(t|x_0)}{dt}. \quad (1)$$

Hence, if we can compute  $S(t|x_0)$  (which is often easier to compute), we obtain  $F(t|x_0)$  simply from Eq. (1). Once we know  $F(t|x_0)$ , the MFPT is just its first moment

$$\langle t_f \rangle(x_0) = \int_0^\infty t F(t|x_0) dt = \int_0^\infty S(t|x_0) dt, \quad (2)$$

where in arriving at the last equality, we substituted Eq. (1) and did integration by parts. Below, we will first compute the survival probability  $S(t|x_0)$  for fixed  $x_0$  and then average over the distribution of  $x_0$ . We will consider the two protocols separately.

## II. PROTOCOL-1: PERIODIC RESETTING TO A RANDOM INITIAL POSITION

We consider an overdamped diffusing particle that starts at an initial position  $x_0$ , which is drawn from a distribution  $\mathcal{P}(x_0)$ . The particle diffuses for a fixed period  $T$  and then its position is instantaneously reset to a new position  $z$ , also drawn from the same distribution  $\mathcal{P}(z)$ . Then the particle diffuses again for a period  $T$ , followed by a reset to a new position  $z'$  drawn from  $\mathcal{P}(z)$  and the process continues. We assume that after each resetting, the reset position  $z$

---

\*E-mail me at: sergio.ciliberto@ens-lyon.fr

is drawn independently from cycle to cycle from the same distribution  $\mathcal{P}(z)$ . We also have a fixed target at a location  $L$ . For fixed  $L$ ,  $T$  and  $\mathcal{P}(z)$ , We want to first compute the mean first-passage time  $\langle t_f \rangle$  to find the target and then optimize (minimize) this quantity with respect to  $T$  (for fixed  $L$  and  $\mathcal{P}(z)$ ). We first compute the MFPT for arbitrary  $\mathcal{P}(z)$  and then focus on the experimentally relevant Gaussian case.

We first recall that for a free diffusing particle, starting at an initial position  $x_0$ , the survival probability that it stays below the level  $L$  up to time  $t$  is given by [6–9]

$$S(t|x_0) = \text{erf} \left( \frac{|L - x_0|}{\sqrt{4Dt}} \right), \quad (3)$$

where  $\text{erf}(z) = (2/\sqrt{\pi}) \int_0^z e^{-u^2} du$  is the error function and  $D$  is the diffusion constant. If the initial position is chosen from a distribution  $\mathcal{P}(x_0)$ , then the survival probability, averaged over the initial position, is given by

$$Q_1(t) = \int_{-\infty}^{\infty} dx_0 \mathcal{P}(x_0) S(t|x_0) = \int_{-\infty}^{\infty} dx_0 \mathcal{P}(x_0) \text{erf} \left( \frac{|L - x_0|}{\sqrt{4Dt}} \right). \quad (4)$$

Now, consider our protocol. Let us compute the survival probability  $Q(t)$  up to time  $t$ , averaged over the distribution of the starting position at the beginning of each cycle. Then it is easy to see the following.

- a)  $0 < t \leq T$ : If the measurement time  $t$  lies in the first cycle of diffusion, then the survival probability upto time  $t$  is simply  $Q_1(t)$  given in Eq. (4), since no resetting has taken place up to  $t$  yet. Note that at the end of the period  $[0, T]$ , the survival probability is simply  $Q_1(T)$ .
- b)  $T < t \leq 2T$ : In this case, the particle has to first survive the period  $[0, T]$  with free diffusion: this occurs with probability  $Q_1(T)$ . Then from time  $T$  till  $T < t \leq 2T$ , it also undergoes a free diffusion but starting from a new reset position  $z$  drawn from  $\mathcal{P}(z)$ . Hence, the survival probability up to  $T < t \leq 2T$  is given by the product of these two events

$$Q_2(t) = Q_1(T) \int_{-\infty}^{\infty} dz \mathcal{P}(z) \text{erf} \left( \frac{|L - z|}{\sqrt{4D(t - T)}} \right). \quad (5)$$

Note that at the end of the cycle

$$Q_2(2T) = Q_1^2(T) \quad (6)$$

where  $Q_1(T)$  is given by Eq. (4).

- c)  $2T < t \leq 3T$ : By repeating the above argument

$$Q_3(t) = Q_1(2T) \int_{-\infty}^{\infty} dz \mathcal{P}(z) \text{erf} \left( \frac{|L - z|}{\sqrt{4D(t - 2T)}} \right) = Q_1^2(T) \int_{-\infty}^{\infty} dz \mathcal{P}(z) \text{erf} \left( \frac{|L - z|}{\sqrt{4D(t - 2T)}} \right) \quad (7)$$

At the end of the 3rd cycle

$$Q_3(3T) = Q_1^3(T) \quad (8)$$

where  $Q_1(T)$  is given by Eq. (4).

- d)  $(n - 1)T < t \leq nT$ : For the  $n$ -th cycle, we have then

$$Q_n(t) = [Q_1(T)]^{n-1} \int_{-\infty}^{\infty} dz \mathcal{P}(z) \text{erf} \left( \frac{|L - z|}{\sqrt{4D(t - (n - 1)T)}} \right) \quad (9)$$

Hence, the survival probability  $Q(t)$  is just  $Q_n(t)$  if  $t$  belongs to the  $n$ -th period, i.e., if  $(n - 1)T < t \leq nT$ , where  $n = 1, 2, \dots$ . In other words, for fixed  $t$ , we need to find the cycle number  $n$  associated to  $t$  and then use the formula for  $Q_n(t)$  in (9). Mathematically speaking

$$Q(t) = \sum_{n=1}^{\infty} Q_n(t) \mathbf{I}_{(n-1)T < t \leq nT} \quad (10)$$

where the indicator function  $I_A = 1$  if the clause  $A$  in the subscript is satisfied and is zero otherwise.

The mean first-passage time  $\langle t_f \rangle$  to location  $L$ , average over the distribution of  $x_0$ , is then given from Eq. (2) as

$$\langle t_f \rangle = \int_0^\infty Q(t) dt \quad (11)$$

where  $Q(t)$  is the survival probability up to time  $t$  in (10). Using the results above for different cycles, we can evaluate this integral in Eq. (11) by dividing the time integral over different cycles. This gives

$$\begin{aligned} \langle t_f \rangle &= \sum_{n=1}^{\infty} \int_{(n-1)T}^{nT} Q_n(t) dt = \sum_{n=1}^{\infty} [Q_1(T)]^{n-1} \int_{(n-1)T}^{nT} dt \int_{-\infty}^{\infty} dz \mathcal{P}(z) \operatorname{erf} \left( \frac{|L-z|}{\sqrt{4D(t-(n-1)T)}} \right) \\ &= \sum_{n=1}^{\infty} [Q_1(T)]^{n-1} \int_0^T d\Delta \int_{-\infty}^{\infty} dz \mathcal{P}(z) \operatorname{erf} \left( \frac{|L-z|}{\sqrt{4D\Delta}} \right), \end{aligned} \quad (12)$$

where in the last line we made a change of variable  $\tau = t - (n-1)T$ . The sum on the right hand side (rhs) of Eq. (12) can be easily performed as a geometric series. This gives

$$\langle t_f \rangle = \frac{\int_0^T d\tau \int_{-\infty}^{\infty} dz \mathcal{P}(z) \operatorname{erf} \left( \frac{|L-z|}{\sqrt{4D\tau}} \right)}{1 - Q_1(T)}. \quad (13)$$

The denominator can be further simplified as

$$1 - Q_1(T) = 1 - \int_{-\infty}^{\infty} dz \mathcal{P}(z) \operatorname{erf} \left( \frac{|L-z|}{\sqrt{4DT}} \right) = \int_{-\infty}^{\infty} dz \mathcal{P}(z) \operatorname{erfc} \left( \frac{|L-z|}{\sqrt{4DT}} \right) \quad (14)$$

where  $\operatorname{erfc}(z) = 1 - \operatorname{erf}(z) = (2/\sqrt{\pi}) \int_z^\infty e^{-u^2} du$  denotes the complementary error function. Note that we have used the normalization:  $\int_{-\infty}^{\infty} \mathcal{P}(z) dz = 1$ . Substituting the result of Eq. (14) in Eq. (13) we get our final formula, valid for arbitrary reset/initial distribution  $\mathcal{P}(z)$

$$\langle t_f \rangle = \frac{\int_0^T d\tau \int_{-\infty}^{\infty} dz \mathcal{P}(z) \operatorname{erf} \left( \frac{|L-z|}{\sqrt{4D\tau}} \right)}{\int_{-\infty}^{\infty} dz \mathcal{P}(z) \operatorname{erfc} \left( \frac{|L-z|}{\sqrt{4DT}} \right)}. \quad (15)$$

The full first-passage probability density  $F(t)$ , averaged over the distribution of  $x_0$ , is then given by

$$F(t) = -\frac{dQ}{dt}, \quad (16)$$

where  $Q(t)$  is given in Eq. (10).

### A. Reset to a Gaussian initial distribution

As an example, let us consider the Gaussian distribution for the reset/initial position

$$\mathcal{P}(x_0) = \frac{1}{\sqrt{2\pi}\sigma^2} e^{-x_0^2/2\sigma^2} \quad (17)$$

where  $\sigma$  denotes the width. In this case, the survival probability  $Q_1(T)$  at the end of the first cycle, is given from Eq. (4) upon setting  $t = T$

$$Q_1(T) = \int_{-\infty}^{\infty} \frac{dx_0}{\sigma\sqrt{2\pi}} e^{-x_0^2/2\sigma^2} \operatorname{erf} \left( \frac{L-x_0}{\sqrt{4DT}} \right). \quad (18)$$

Let us introduce two dimensionless constants  $b$  and  $c$

$$b = \frac{L}{\sigma}; \quad c = \frac{L}{\sqrt{4DT}}. \quad (19)$$

Then in terms of these two constants, Eq. (18), after suitable rescaling, can be simplified to

$$Q_1(T) = \frac{b}{\sqrt{2\pi}} \int_{-\infty}^{\infty} dy e^{-b^2 y^2/2} \operatorname{erf}(c|1-y|). \quad (20)$$

Note that in the limit of  $b \rightarrow \infty$ , i.e., when  $L \ll \sigma$  (corresponding to resetting to the origin) one gets

$$Q_1(T) \Big|_{b \rightarrow \infty} = \operatorname{erf}(c), \quad (21)$$

where we used  $(b/\sqrt{2\pi}) e^{-b^2 y^2/2} \rightarrow \delta(y)$  when  $b \rightarrow \infty$ .

### 1. Mean first-passage time

Substituting the Gaussian  $\mathcal{P}(z)$  in Eq. (15), and rescaling  $\tau = vT$  we can write everything in dimensionless form

$$\tau = \frac{4D\langle t_f \rangle}{L^2} = \frac{\int_0^1 dv \int_{-\infty}^{\infty} du e^{-u^2/2} \operatorname{erf}\left(\frac{c}{\sqrt{v}}|1-u/b|\right)}{c^2 \int_{-\infty}^{\infty} du e^{-u^2/2} \operatorname{erfc}(c|1-u/b|)} \equiv w(b, c) \quad (22)$$

where the dimensionless constants  $b$  and  $c$  are given in Eq. (19). It is hard to obtain a more explicit expression for the function  $w(b, c)$  in Eq. (22). But it can be easily evaluated numerically.

To make further analytical progress, we first consider the limit  $\sigma \rightarrow 0$ , i.e.,  $b = L/\sigma \rightarrow \infty$ . In this limit, the reset distribution  $\mathcal{P}(z) \rightarrow \delta(z)$ . Hence, Eq. (15) or equivalently Eq. (22) simplifies considerably and the integrals can be evaluated explicitly. We obtain an exact expression

$$\tau = \frac{4D\langle t_f \rangle}{L^2} = \frac{\operatorname{erf}(c) + 2c \left( e^{-c^2}/\sqrt{\pi} - c \operatorname{erfc}(c) \right)}{c^2 \operatorname{erfc}(c)} \equiv w(b \rightarrow \infty, c) \equiv w(c) \quad (23)$$

where we recall  $c = L/\sqrt{4DT}$ . In Fig. 2 of the main text, we plot the function  $w(c)$  vs.  $c$ , which has a minimum at

$$c_{\text{opt}} = 0.738412\dots \quad (24)$$

At this optimal value,  $\tau_{\text{opt}} = w(c_{\text{opt}}) = 5.34354\dots$ . Hence, the optimal mean first-passage time to find the target located at  $L$  is given by

$$\langle t_f \rangle_{\text{opt}} = (5.34354\dots) \frac{L^2}{4D}. \quad (25)$$

Note that this result is true in the limit  $b = L/\sigma \rightarrow \infty$ , i.e., when the target is very far away from the starting/resetting position. In this limit, our result coincides with Ref. [3] where the authors studied periodic resetting to the fixed initial position  $x_0 = 0$  by a different method. This is expected since the limit  $b = L/\sigma \rightarrow \infty$  limit is equivalent to  $\sigma \rightarrow 0$  (with fixed  $L$ ) and one would expect to recover the fixed initial position results.

But the most interesting and unexpected result occurs for finite  $b$ . In this case we can evaluate the rhs of Eq. (22) numerically. This has been done to plot the continuous lines in Fig. 3 of the main text, which shows the existence of a metastable minimum for  $b > b_c \simeq 2.3$

### 2. Full first-passage probability density $F(t)$

The first-passage probability density can be computed from Eq. (16) and is plotted in Fig. 2 of the main text. For a finite  $b = L/\sigma$  we see those spectacular spikes at the beginning of each cycle. In this subsection, we analyse the origin of these spikes. For this let us analyse the survival probability  $Q_n(t)$  in Eq. (9) close to the epoch  $nT$ , i.e., when the  $n$ -th period ends. We set  $t = nT + \Delta$  where  $\Delta$  is small. For  $\Delta > 0$ , we are in the  $(n+1)$ -th cycle, while for  $\Delta < 0$  we are in the  $n$ -th cycle. We consider the  $\Delta > 0$  and  $\Delta < 0$  cases separately.

**The case  $\Delta > 0$ :** Since  $t = nT + \Delta$  with  $\Delta > 0$  small,  $t$  now belongs to the  $(n+1)$ -th cycle, so we replace  $n$  by  $n+1$  in Eq. (9) and get

$$Q_{n+1}(t = nT + \Delta) = [Q_1(T)]^n \int_{-\infty}^{\infty} \frac{dz}{\sigma\sqrt{2\pi}} e^{-z^2/2\sigma^2} \operatorname{erf}\left(\frac{|L-z|}{\sqrt{4D\Delta}}\right), \quad (26)$$

where  $Q_1(T)$  is given in Eq. (20). It is convenient first to use the relation  $\operatorname{erf}(z) = 1 - \operatorname{erfc}(z)$  and rewrite this as

$$Q_{n+1}(t = nT + \Delta) = [Q_1(T)]^n \left[ 1 - \int_{-\infty}^{\infty} \frac{dz}{\sigma \sqrt{2\pi}} e^{-z^2/2\sigma^2} \operatorname{erfc} \left( \frac{|L-z|}{\sqrt{4D\Delta}} \right) \right] \quad (27)$$

To derive the small  $\Delta$  asymptotics, we make a change of variable  $(L-z)/\sqrt{4D\Delta} = y$  on the rhs of Eq. (27). This leads to, using  $b = L/\sigma$ ,

$$Q_{n+1}(t = nT + \Delta) = [Q_1(T)]^n \left[ 1 - \frac{\sqrt{4D\Delta}}{L} \frac{b}{\sqrt{2\pi}} \int_{-\infty}^{\infty} dy e^{-\frac{b^2}{2}(1-\sqrt{4D\Delta}y/L)^2} \operatorname{erfc}(|y|) \right]. \quad (28)$$

We can now make the limit  $\Delta \rightarrow 0$ . To leading order in  $\Delta$ , we can set  $\Delta = 0$  inside the exponential in the integrand on the rhs and using  $\int_{-\infty}^{\infty} dy \operatorname{erfc}(|y|) = 2/\sqrt{\pi}$  we get

$$Q_{n+1}(t = nT + \Delta) \simeq [Q_1(T)]^n \left[ 1 - A_+(b) \sqrt{\Delta} \right], \quad A_+(b) = \sqrt{\frac{8D}{\pi^2 L^2}} b e^{-b^2/2}. \quad (29)$$

Taking derivative with respect to time, i.e., with respect  $\Delta$ , we find that as  $\Delta \rightarrow 0^+$ , the first-passage probability density  $F(t) = -dQ/dt$  diverges for any finite  $b$  as

$$F(t = nT + \Delta) \simeq \frac{A_n(b)}{\sqrt{\Delta}} \quad (30)$$

where the amplitude  $A_n(b)$  of the inverse square root divergence is given by the exact formula

$$A_n(b) = \sqrt{\frac{2D}{\pi^2 L^2}} b e^{-b^2/2} [Q_1(T)]^n \quad (31)$$

where  $Q_1(T)$  (which also depends on  $b$ ) is given in Eq. (20). This inverse square root divergence at the beginning of any cycle, for any finite  $b$ , describes the spikes in Fig. 2 of the main text. Note that the amplitude  $A_n(b)$  of the  $n$ -th spike in Eq. (31) decreases exponentially with  $n$ , as seen also in Fig. 2 of the main text.

Interestingly, we see from Eq. (31) that the amplitudes of the spikes decrease extremely fast as  $b$  increases and the spikes disappear in the  $b \rightarrow \infty$  limit. Since  $b = L/\sigma$ , we see that the limit  $b \rightarrow \infty$  corresponds to  $\sigma \rightarrow 0$  limit (for fixed  $L$ ). This is indeed the case where one resets always to the origin. In fact, if we first take the limit  $b \rightarrow \infty$  keeping  $\Delta$  fixed and then take the limit  $\Delta \rightarrow 0$ , we get a very different result. Taking  $b \rightarrow \infty$  limit first in Eq. (28) we get,

$$Q_{n+1}(t = nT + \Delta) \Big|_{b \rightarrow \infty} = [Q_1(T)]^n \left[ 1 - \operatorname{erfc} \left( \frac{L}{\sqrt{4D\Delta}} \right) \right], \quad (32)$$

where  $Q_1(T)$  now is given in Eq. (21). Taking a derivative with respect  $t$ , i.e., with respect to  $\Delta$ , we get the first-passage probability density

$$F(t = nT + \Delta) \Big|_{b \rightarrow \infty} = [Q_1(T)]^n \frac{L}{\sqrt{4\pi D \Delta^3}} e^{-L^2/(4D\Delta)}. \quad (33)$$

Thus, in the  $b \rightarrow \infty$  limit, the first passage probability actually vanishes extremely rapidly as  $\Delta \rightarrow 0$  due to the essential singular term  $\sim e^{-L^2/(4D\Delta)}$ .

To summarize, the behavior of the first-passage probability density at the beginning of the  $n$ -th period is strikingly different for  $\sigma = 0$  ( $b \rightarrow \infty$ ) and  $\sigma > 0$  ( $b$  finite): in the former case it vanishes extremely rapidly as  $t \rightarrow nT$  from above, while in the latter case it diverges as an inverse square root leading to a spike at the beginning of each period. Thus the occurrence of spikes for  $\sigma > 0$  is a very clear signature of the finiteness of  $\sigma$ . Physically, a spike occurs because if  $\sigma$  is finite, immediately after each resetting the searcher may be very close to the target and has a finite probability of finding the target immediately without further diffusion.

**The case  $\Delta < 0$ :** When  $t = nT + \Delta$  with  $\Delta < 0$ , the effects are not so prominent as in the  $\Delta > 0$  case. For  $\Delta < 0$ , since  $t$  belongs to the  $n$ -th branch, we consider the formula in Eq. (9) with  $n$  and get

$$Q_n(t = nT + \Delta) = [Q_1(T)]^{n-1} \int_{-\infty}^{\infty} \frac{dz}{\sigma \sqrt{2\pi}} e^{-z^2/2\sigma^2} \operatorname{erf} \left( \frac{|L-z|}{\sqrt{4D(T+\Delta)}} \right). \quad (34)$$

Now taking the  $\Delta \rightarrow 0$  limit in Eq. (34) is straightforward since there is no singular behavior. Just Taylor expanding the error function for small  $\Delta$  up to  $O(\Delta)$ , and making the change of variable  $(L - z)/\sqrt{4DT} = y$ , we obtain

$$Q_n(t = nT + \Delta) = [Q_1(T)]^n - \Delta B_n(b) + O(\Delta^2), \quad (35)$$

where the constant

$$B_n(b) = \frac{b [Q_1(T)]^{n-1}}{cT\pi\sqrt{2}} \int_{-\infty}^{\infty} dy |y| e^{-y^2} e^{-\frac{b^2}{2}(1-cy)^2}, \quad (36)$$

with  $c = L/\sqrt{4DT}$ . Taking derivative with respect to  $\Delta$  in Eq. (35) gives the leading behavior of the first-passage probability density: it approaches a constant as  $\Delta \rightarrow 0$

$$F(t = nT + \Delta) \simeq B_n(b). \quad (37)$$

One can easily check that even in the  $b \rightarrow \infty$  limit, this constant remains nonzero and is given by

$$F(t = nT + \Delta) \Big|_{b \rightarrow \infty} \simeq \frac{[Q_1(T)]^{n-1}}{\sqrt{\pi} T c^3} e^{-1/(2c^2)}, \quad (38)$$

where  $Q_1(T)$  is now given in Eq. (21). Thus, for any  $\sigma \geq 0$ , as one approaches the epoch  $t = nT$  from the left, i.e., at the end of the  $(n-1)$ -th cycle, the first-passage probability density approaches a constant  $B_n(b)$  given in Eq. (36). This constant remains finite even when  $b \rightarrow \infty$ . On this side, there is no spectacular effect distinguishing  $\sigma = 0$  ( $b \rightarrow \infty$ ) and  $\sigma > 0$  (finite  $b$ ), as is the case on the right side of the epoch  $nT$ . On the right, for finite  $b$  we have an inverse square root divergence as in (30), while for  $b \rightarrow \infty$ , it vanishes rapidly as  $\Delta \rightarrow 0$ . Thus in the large  $b$  limit, we have a discontinuity or drop from left to right (not a spike) as we see in the inset of Fig. 2 in the main text.

### III. PROTOCOL-2: RANDOM RESETTING TO A RANDOM INITIAL POSITION

We consider an overdamped diffusing particle that starts at an initial position  $x_0$ , which is drawn from a distribution  $\mathcal{P}(x_0)$ . The particle diffuses for a random interval  $T$  drawn from an exponential distribution  $P(T) = r e^{-rT}$  and then its position is instantaneously reset to a new position  $z$ , also drawn from the same initial distribution  $\mathcal{P}(z)$ . Then the particle diffuses again for another random interval  $T$  (again drawn from the exponential distribution  $P(T)$ ), followed by a reset to a new position  $z'$  drawn from  $\mathcal{P}(z)$  and the process continues. We assume that after each resetting, the reset position  $z$  is drawn independently from cycle to cycle from the same distribution  $\mathcal{P}(z)$ . Similarly, the interval  $T$  is also drawn independently from cycle to cycle from the same distribution  $P(T) = r e^{-rT}$ . We also have a fixed target at a location  $L$ . For fixed  $L$ ,  $r$  and  $\mathcal{P}(z)$ , We want to first compute the mean first-passage time  $\langle t_f \rangle$  to find the target and then optimize (minimize) this quantity with respect to  $r$  (for fixed  $L$  and  $\mathcal{P}(z)$ ). Recall that in protocol-1, we just had a fixed  $T$ , but in protocol-2  $T$  is exponentially distributed.

In this case, the mean first-passage time  $\langle t_f \rangle$  has a simple closed formula. This formula can be derived following steps similar to those in Ref. [2]. Skipping further details, we find

$$\langle t_f \rangle = \frac{1}{r} \left[ \frac{1}{\int_{-\infty}^{\infty} dz \mathcal{P}(z) \exp(-\sqrt{\frac{r}{D}} |L - z|)} - 1 \right]. \quad (39)$$

Consider the special case of Gaussian distribution of Eq. (17) Substituting this Gaussian  $\mathcal{P}(z)$  in Eq. (39), and performing the integral explicitly, we get the dimensionless mean first-passage time

$$\tau = \frac{4D\langle t_f \rangle}{L^2} = \frac{4}{c^2} \left[ \frac{2e^{-c^2/2b^2}}{e^c \operatorname{erfc}\left(\frac{1}{\sqrt{2}}\left(\frac{c}{b} + b\right)\right) + e^{-c} \operatorname{erfc}\left(\frac{1}{\sqrt{2}}\left(\frac{c}{b} - b\right)\right)} - 1 \right] \equiv w_2(b, c) \quad (40)$$

where the dimensionless constants  $b$  and  $c$  are given by

$$b = \frac{L}{\sigma}; \quad c = \sqrt{\frac{r}{D}} L. \quad (41)$$

Recall that in periodic protocol (with a fixed  $T$  discussed in section II A) , the parameter  $b = L/\sigma$  is the same, but the parameter  $c = L/\sqrt{4DT}$  is different. In protocol-2, the reset rate  $r$  effectively plays the role of  $1/T$  in protocol-1.

The formula for  $w_2(b, c)$  in Eq. (40) for protocol-2 is simpler and more explicit, compared to the equivalent formula Eq.22 for protocol-1.

In Eq. (40), consider first the limit  $b \rightarrow \infty$ , i.e., resetting to a fixed initial condition. In this case, Eq. (40) reduces precisely to the formula derived by Evans and Majumdar [1]

$$\tau = w_2(b \rightarrow \infty, c) = \frac{4}{c^2} [e^c - 1] . \quad (42)$$

In this  $b \rightarrow \infty$  limit,  $\tau$  as a function of  $c$ , has a unique minimum at  $c = c^* = 1.59362\dots$ , where  $\tau(c = c^*) = 6.17655\dots$

For finite fixed  $b$ , it is very easy to plot the function  $w_2(b, c)$  vs.  $c$  given in Eq. (40) and one finds that as in protocol-1,  $w_2(b, c)$  first decreases with increasing  $c$ , achieves a minimum at certain  $c_1(b)$ , then starts increasing again—becomes a maximum at  $c_2(b)$  and finally decreases for large  $c$  as  $\sim 1/c$  (this asymptotics for large  $c$  can be computed exactly from Eq. (40)). Note that the actual values of  $c_1(b)$  and  $c_2(b)$  are of course different in the two protocols. Interestingly, this metastable optimum time at  $c = c_1(b)$  disappears when  $b$  becomes smaller than a critical value  $b_c = 2.53884$ . For  $b < b_c$ , the function  $w_2(b, c)$  decreases monotonically with increasing  $c$ . Hence, for  $b < b_c$ , the best solution is  $c = \infty$  (i.e., repeated resetting). The curves plotted in Fig. 4 of the main text correspond to this theoretical prediction and they have been checked experimentally and numerically. This numerical test allows us to clearly state that the small disagreement at small  $b$  and large  $c$  of the experimental data with the theoretical predictions is due to the maximum sampling rate of our analog to digital converter which was not fast enough to detect very short MFPT.

- 
- [1] M. R. Evans and S. N. Majumdar, Phys. Rev. Lett. **106**, 160601 (2011).
  - [2] M. R. Evans and S. N. Majumdar, J. Phys. A: Math. Theor. **44**, 435001 (2011).
  - [3] A. Pal, A. Kundu, and M. R. Evans, J. Phys. A: Math. Theor. **49**, 225001 (2016).
  - [4] U. Bhat, C. De Bacco, and S. Redner, J. Stat. Mech. **083401** (2016).
  - [5] M. R. Evans, S. N. Majumdar, and G. Schehr, J. Phys. A: Math. Theor. **53**, 193001 (2020).
  - [6] S. N. Majumdar, Curr. Sci. **77**, 370 (1999).
  - [7] S. Redner, *A guide to first-passage processes*, Cambridge University Press (2001).
  - [8] S. N. Majumdar, Physica A, **389**, 4299 (2010).
  - [9] A. J. Bray, S. N. Majumdar, and G. Schehr, Adv. in Phys. **62**, 225 (2013).